Large wavelength magnetic modulation in (0001)Tb films

1999 J. Phys.: Condens. Matter 11 L497

(http://iopscience.iop.org/0953-8984/11/44/101)

J. Phys.: Condens. Matter **11** (1999) L497–L503. Printed in the UK PII: S0953-8984(99)06476-0

LETTER TO THE EDITOR

Large wavelength magnetic modulation in (0001)Tb films

C Dufour†, K Dumesnil†, A Mougin†, Ph Mangin† and M Hennion‡

† Laboratoire de Physique des Matériaux, Université H Poincaré-Nancy I, BP 239, 54506 Vandoeuvre les Nancy Cédex, France

‡ Laboratoire Léon Brillouin, Centre d'Etudes Nucléaires de Saclay, 91191 Gif sur Yvette, France

Received 30 July 1999

Abstract. A large wavelength magnetic modulation, which has never been observed up to now, has been evidenced by neutron scattering experiments in (0001) terbium single crystal films. With decreasing temperature, this magnetic arrangement appears when the helical one vanishes and before the long range ferromagnetic order sets in. The large wavelength magnetic modulation is squared and it varies between 180 and 700 Å depending on the temperature and the film thickness. We assume that it is due to the stacking of ferromagnetic blocks whose net magnetization points along a basal plane direction and rotates by a given angle between two consecutive blocks. The occurrence of this phase seems to be independent of the strains induced by epitaxy but it would be related to the lattice clamping between epitaxied layers. A temperature–magnetic field phase diagram of a terbium film is presented.

The magnetic structure of bulk terbium was explored three decades ago by neutron scattering [1–4] and recently by resonant magnetic x-ray scattering [5, 6]. Bulk terbium orders magnetically at $T_N = 230$ K, where it exhibits an helical phase whose wave vector is parallel to the c-axis of the hexagonal compact structure. In this helical phase, the magnetic moments lie in the basal planes and are ferromagnetically ordered in each individual plane. The generalized susceptibility $\chi(q)$ of the conduction electrons is maximum for a wave vector $q_m = 0.22\pi/c$, and, correlatively, the turn angle between magnetic moments of successive basal planes is 21° just below T_N. This helical phase is stable on a very reduced temperature range: a first order ferromagnetic transition occurs at $T_C = 220$ K and the turn angle then drops discontinuously to zero. Because of the shape of the electronic cloud and of the consequent anisotropy, the magnetic moments lie in the basal plane along the b axis. The ferromagnetic transition is acknowledged to be driven by magnetoelastic effects [7] which balance the exchange interaction provided by the conduction electrons. In the paramagnetic phase, the neutron diffraction peaks are purely nuclear and the magnetic scattering is diffuse. The diffraction pattern collected in the helical phase is characterized by the occurrence of satellites located at $\pm q_m$ from the nuclear peaks and the ferromagnetic transition leads to the disappearance of these satellites and to the simultaneous increase of the nuclear peaks intensity. Resonant magnetic x-ray scattering studies confirmed the neutron observations and did not show any lock-in behaviour along the easy anisotropy axis in the helical phase, probably because of the weak anisotropy terms, so close to the ordering temperature in terbium [5].

Recently, the success of molecular beam epitaxy techniques has considerably renewed the research in the field of magnetism of rare earth thin films and superlattices. Fascinating behaviours such as the propagation of the magnetic helix through non-magnetic or paramagnetic layers, antiferromagnetic coupling between ferromagnetic layers and very large

0953-8984/99/440497+07$30.00

shifts of Curie temperature have been observed [8–10]. These effects have been attributed to the long range polarization of conduction electrons, which are considered to be responsible for the magnetic coupling, and to the epitaxial strains, which bring a significant contribution to the magnetoelastic energy and thus modify the energy balance between ferromagnetic and helical phases.

In this paper, we present the evidence of an original magnetic arrangement in epitaxial (0001) terbium thin films. The transition from the helical phase to the long range ferromagnetic order is not direct as in bulk terbium but occurs via the development of a stacking of ferromagnetic blocks, whose resulting magnetization rotates with a wave vector parallel to the *c* axis.

The samples have been prepared by molecular beam epitaxy in a vacuum chamber whose base pressure was about 4×10^{-11} Torr. They were grown upon a $(11\bar{2}0)$ sapphire substrate which had been submitted to a degreasing treatment and which had been heated to 850 °C in one hour in the growth chamber. Following the method proposed by Kwo *et al* [11], the substrate was first covered by a 500 Å niobium buffer deposited at 820 °C. Terbium and yttrium were then evaporated from electron guns and deposited onto the substrate kept at 400 °C, in order to allow surface mobility, while limiting interfacial interdiffusion. The deposition rate, calibrated using a quartz crystal monitor and an optical sensor, was 0.5 Å s^{-1}. The epitaxial relationships along the growth direction are $(11\bar{2}0)$ Al_2O_3 ∥ (110)Nb ∥ (0001) Tb and Y. Terbium films are either deposited on niobium (sample A has a terbium thickness of 7000 Å and sample B a terbium thickness of 2000 Å) or sandwiched between two 500 Å yttrium layers (sample C has a terbium thickness of 400 Å).

The structural quality of these samples has been checked by *in situ* RHEED observations and then by large angle x-ray scattering experiments. The RHEED patterns exhibit thin and continuous streaks which reveal a good crystalline quality of the samples. The large angle x-ray scattering patterns collected with the wave-vector transfer along $\boldsymbol{c}^*$ permit us to determine the terbium *c* parameter. It is very close to the bulk value in the thick A and B films but is 0.4% smaller in the C film because of the strain due to the epitaxy on yttrium. The full width at half maximum of the rocking curve through the (0002) Bragg peak gives a mosaic spread of approximately 0.2° in these samples.

The magnetic properties have been mainly investigated by neutron diffraction experiments performed on the G4.3 triple-axis spectrometer at LLB (Saclay, France). The incident neutron wavelength was 4.245 Å and the collimations in front and beyond the monochromator and the analyser were 60′, 30′, 30′ and 30′, yielding an elastic resolution width of 0.008 $Å^{-1}$. The samples were mounted in a closed-cycle cryostat that enabled the spectra to be collected between 10 K and room temperature. Neutron diffraction experiments were also performed under an external magnetic field (maximal intensity of 1 T), vertically oriented in the sample plane.

Neutron scattering spectra collected under zero magnetic field from the 7000 Å thick terbium film (sample A) are shown in figure 1(a) for temperatures between 230 and 216 K and in figure 1(b) for temperatures between 214 and 20 K. At 230 K, the neutron diffraction pattern exhibits the (0002) nuclear peak at $q = 2.21$ $Å^{-1}$. Around 229 K, two satellites (referred to as 'helix' in figure 1(a)) emerge on each side of the (0002) peak. These satellites are due to the well known magnetic helix which develops in bulk terbium with a wave vector parallel to the *c* axis. Because their intensity is related to the square of the average magnetic moments, it increases continuously when the temperature decreases. The helix is stable down to about 220 K; then the satellites intensity drops abruptly over about 2 K. This behaviour is similar to the one observed in bulk terbium. However, in contrast to bulk terbium, the magnetic intensity is not directly transferred from the helix satellites to the (0002) Bragg peak but it is transferred

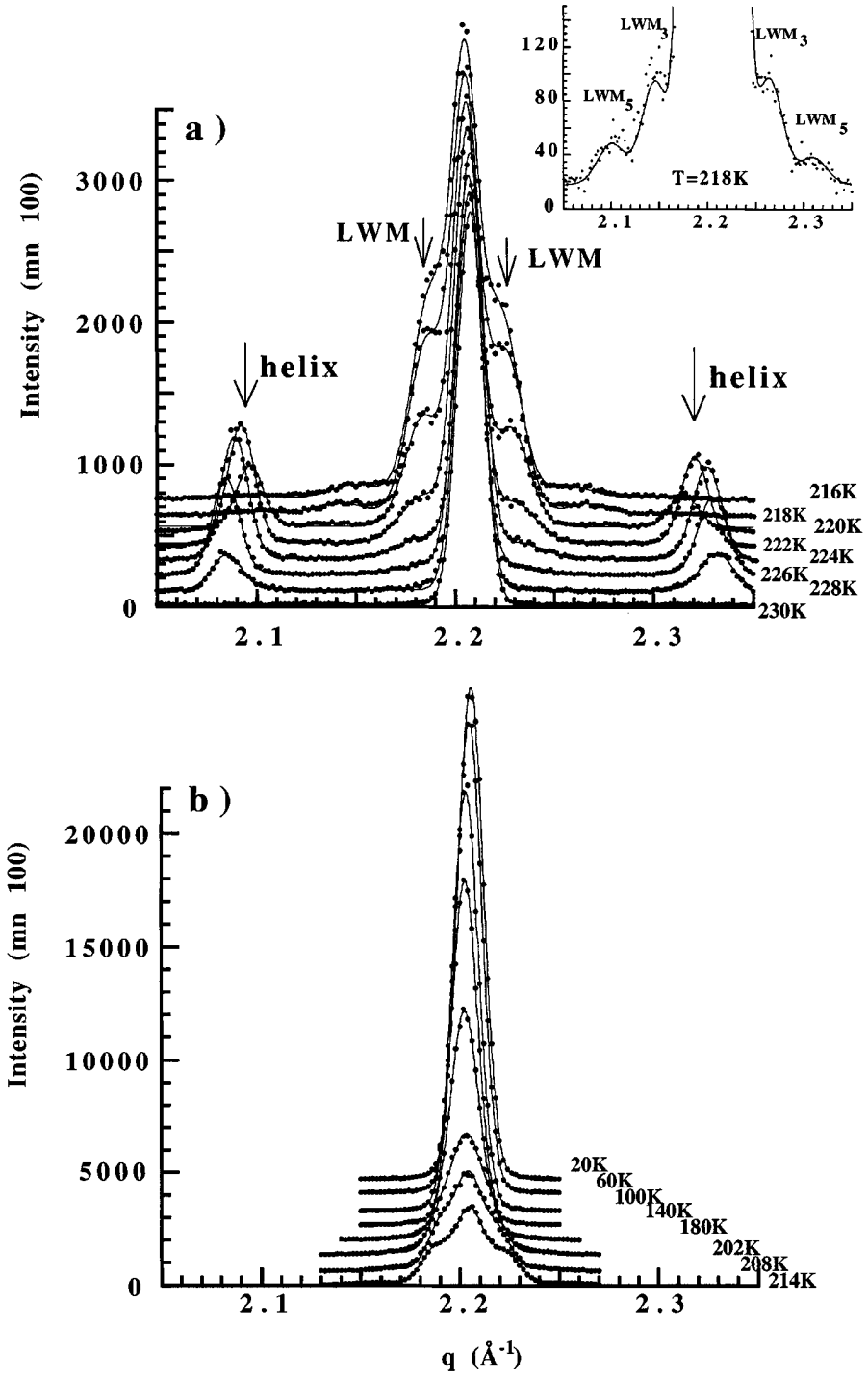

Figure 1. Neutron scattering spectra collected at different temperatures along the c^* direction around the (0002) reflection for a 7000 Å thick terbium film: (a) $T = 230$, 228, 226, 224, 222, 220, 218 and 216 K from the bottom to the top; (b) $T = 214$, 208, 202, 180, 140, 100, 60 and 20 K from the bottom to the top. The inset shows the occurrence of the third and fifth order satellites of the LWM phase at 218 K.

to a new set of satellites. These satellites are very close to the (0002) Bragg peak, but far away enough to keep the intensity of this peak unchanged. They reveal an unexpected magnetic modulation of small wave vector and therefore of large wavelength, which can be estimated to 290 Å at 220 K. The intensity of these large wavelength modulation peaks (referred to as LWM in figure 1) increases when the temperature decreases. At 222 and 220 K, there is clearly coexistence of both magnetic modulations: the classical helical modulation and the large wavelength modulation.

Table 1. Temperature range of existence of the magnetic phases in terbium for three different samples.

Sample	Helical phase	Long wavelength modulation (LWM)
A: 7000 Å Tb	230–220 K	224–180 K
B: 2000 Å Tb	230–220 K	225–180 K
C: Y/400 Å Tb/Y	228–160 K	170–130 K

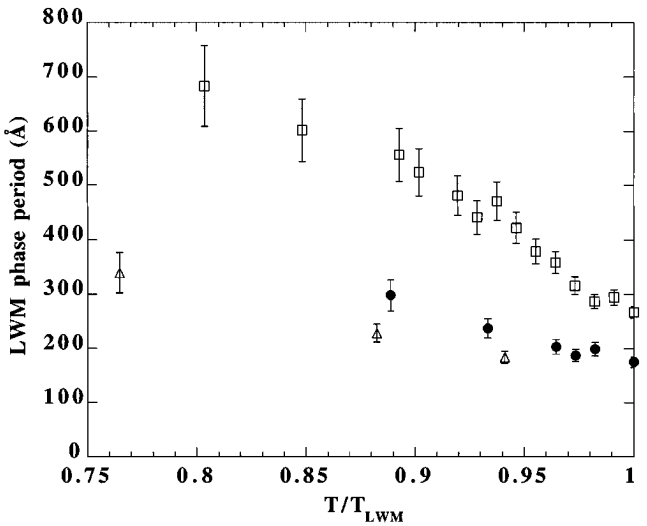

Figure 2. Variation of the large wavelength magnetic modulation for 7000 (open squares), 2000 (filled circles) and 400 Å (open triangles) terbium films as a function of the reduced temperature T/T_{LWM} (T_{LWM} is the temperature of appearance of the LWM phase).

A careful examination of the diffraction pattern collected at 218 K shows that the large wavelength modulation gives rise to several other additional satellites referred to as LWM_3 and LWM_5 in the inset of figure 1(a). These peaks are at the position $q_{Bragg} \pm (2n + 1)Q_{LWM}$ (n is an integer and Q_{LWM} is the wave vector of the large wavelength modulation). This reveals that the modulation is not sinusoidal but has a square shape, which is known to give rise to such odd satellites.

When the temperature decreases, the LWM main satellites become closer and closer to the (0002) peak and progressively merge into that peak. This last process is clearly visible from 214 to 208 K (figure 1(b)) and, below this temperature, it continues to be manifest by the simultaneous increase of the (0002) peak intensity and the reduction of its width. Below 180 K, the width of the Bragg peak remains constant down to low temperature: the sample

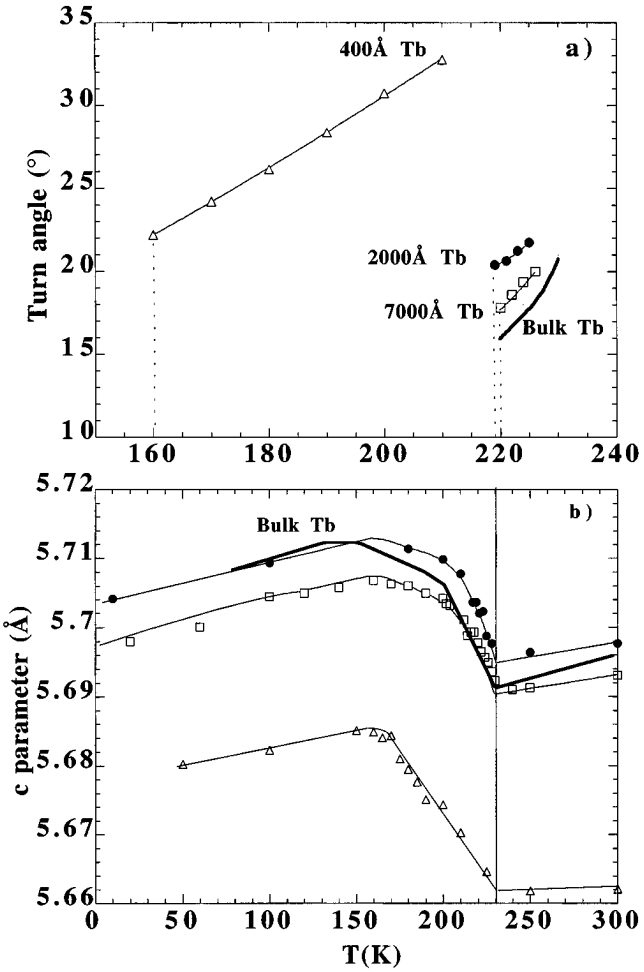

Figure 3. Thermal variation of the terbium turn angle (a) and of the terbium c parameter (b) for 7000 (open squares), 2000 (filled circles) and 400 Å (open triangles) terbium films.

presents a long range ferromagnetic order. When increasing the temperature again, the process is reversible: the LWM and helical modulation successively reappear. However, the results present some hysteresis, as expected from a first order transition.

A very similar behaviour was observed from the samples B and C. However, the 400 Å thick terbium film deposited between two yttrium layers (film C) exhibits successive phases with a shift of the transition temperatures. In this thin film, the helical phase is stable from 228 to 160 K and the LWM phase is present from 170 down to 130 K. The temperature ranges of existence of both magnetic phases (helical and large wavelength modulations) are summarized in table 1. The LWM period deduced from the position of the satellites is reported in figure 2 for samples A, B and C, as a function of T/T_{LWM} (T_{LWM} is the temperature of appearance of the LWM phase). For all the samples, the LWM magnetic period increases when the temperature decreases. It presents the same stability range in reduced temperature unit (experimental points for $T/T_{LWM} < 0.88$ have not been measured for sample B). The LWM period appears to be smaller for thinner films.

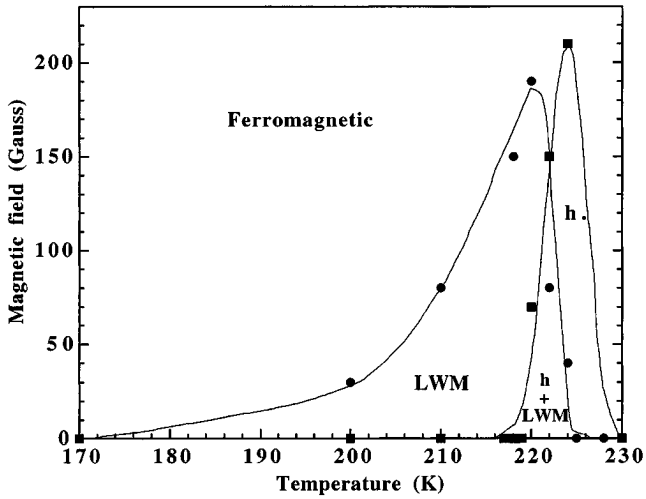

Figure 4. Magnetic phase diagram deduced from neutron diffraction data for the 7000 Å thick terbium film (h.: helical phase; LWM: large wavelength modulation phase).

The larger stability of the helical phase (i.e. the decrease of T_C) in sample C is consistent with the reduced c parameter due to the epitaxial strains, which increase the in-plane parameters of terbium deposited between yttrium layers. Correlatively, the turn angle is enhanced in agreement with the relation between the turn angle and the stability of the helical phase [12]. Evolutions of the c parameters and of the turn angles are reported in figure 3.

Finally, we have determined the stability of both magnetic modulations under an external magnetic field. The modulated phases are progressively replaced by a field-induced long range ferromagnetic order. The magnetic field needed to destroy the LWM phase is of the same order of magnitude as the one necessary to destroy the helical phase. The magnetic phase diagram versus temperature and magnetic field for the 7000 Å Tb film is reported in figure 4.

It should be noticed that such an LWM phase has also been observed in (0001) Dy_xTb_{1-x} films with $x = 0.2$, 0.55 and 0.78, whereas it has never been observed in pure dysprosium films prepared in similar conditions.

Concerning the origin of this LWM phase, we suggest that it is constituted by the stacking along the c axis of ferromagnetic blocks with in-plane magnetization. Assuming that the resulting moment in each block is aligned along one of the equivalent b easy axes and that the magnetization rotates by 60° between two consecutive blocks, we can deduce the block thickness from the magnetic period. In the 7000 Å film, the block thickness would increase from 15 to 41 atomic planes when the temperature decreases. The main argument for this block rotation is the occurrence of third and fifth order harmonics that we observed in sample A at 218 and 216 K (inset of figure 1(a)) and which are typical of a square profile. This magnetic arrangement permits us to obtain a compromise between the lowest energy configuration in the terbium film, that would be the long range ferromagnetic order accompanied by magnetostrictive lattice strains, and a configuration limiting the lattice strains in the other non-magnetic layers; the strains in these layers would namely only lead to a cost in elastic energy. Because of the clamping between the terbium and the non-magnetic buffer lattices, a long range ferromagnetic order would then increase the total elastic energy in the sample. The 'block by block' rotation of the magnetization permits us to keep the short range ferromagnetic ordering for most of the atoms in terbium and to reduce the total elastic energy.

When the temperature decreases, the magnetic anisotropy becomes stronger and no longer allows the existence of domain walls between the ferromagnetic blocks. This drives the long range ferromagnetic arrangement. In the same way, the LWM phase is not observed in pure dysprosium film because of the larger magnetic anisotropy of dysprosium at the ferromagnetic transition.

In summary, we have demonstrated the existence of a new large wavelength modulation phase in terbium single crystalline films. The occurrence of this phase is independent of the strains induced by epitaxy but would be related to the clamping between epitaxied layers. In dysprosium films, it was established that the magnetic phase diagram is tuned almost entirely by the basal plane strain and that the lattice clamping has a relatively small effect on the magnetic behaviour [13]. From the results presented in this letter one can conclude that, in terbium films, two effects are observed: (i) the epitaxial strains lead to a reduction of the Curie temperature as in dysprosium films; (ii) the lattice clamping also modifies the magnetic phase diagram by inducing a new magnetic order; this magnetic order can occur because magnetic anisotropy in terbium is smaller than in dysprosium in the helical–ferromagnetic transition temperature range.

References

[1] Koehler W C, Child H R, Wollan E O and Cable J W 1963 *J. Appl. Phys. Suppl.* **34** 1335
[2] Koehler W C 1965 *J. Appl. Phys.* **36** 1078
[3] Dietrich O W and Als-Nielsen J 1967 *Phys. Rev.* **162** 315
[4] Umebayashi H, Shirane G, Frazer B C and Daniels W B 1968 *Phys. Rev.* B **165** 688
[5] Gehring P M, Rebelsky L, Gibbs D and Shirane G 1992 *Phys. Rev.* B **45** 243
[6] Tang C C, Stirling W G, Jones D L, Wilson C C, Haycock P W, Rollason A J, Thomas A H and Fort D 1992 *J. Magn. Magn. Mater.* **103** 86
[7] Coqblin B 1997 *The Electronic Structure of the Rare Earth Metals and Alloys: the Heavy Rare Earth* (London: Academic)
[8] Erwin R W, Rhyne J J, Salamon M B, Borchers J, Sinha S, Du R, Cunningham J E and Flynn C P 1987 *Phys. Rev.* B **35** 6806
[9] Dumesnil K, Dufour C, Mangin Ph, Marchal G and Hennion M 1996 *Phys. Rev.* B **54** 6407
[10] Cowley R A 1998 *J. Magn. Magn. Mater.* **177–181** 1156 and references therein
[11] Kwo J, Hong M and Nakahara S 1986 *Appl. Phys. Lett.* **49** 349
[12] Dufour C, Dumesnil K, Mougin A, Mangin Ph, Marchal G and Hennion M 1997 *J. Phys.: Condens. Matter* **9** L131
[13] Tsui F and Flynn C P 1993 *Phys. Rev. Lett.* **71** 1462